DOI: 10.5505/2023geoteknik.SS-03

LIQUEFACTION-INDUCED FAILURE OF DEMİRKÖPRÜ BRIDGE PILE FOUNDATION AND RETAINING SYSTEM FOLLOWING THE FEBRUARY 6, 2023 KAHRAMANMARAŞ EARTHQUAKE SEQUENCE

6 ŞUBAT KAHRAMANMARAŞ DEPREMLERİ SONRASI DEMİRKÖPRÜ KAZIKLI TEMEL ELEMANLARI VE DAYANMA YAPILARINDA GÖRÜLEN ZEMİN SIVILAŞMASI SEBEPLİ YENİLMELER

Soner OCAK[1] and Kemal Onder Cetin[2]

ABSTRACT

Liquefaction-induced failure of Demirköprü bridge, more specifically the rotational failure of the piled foundations and the retaining system of the eastern abutment, was discussed. The soil liquefaction triggering assessment results suggested that the silty sand layer located at depth range of 8.0 to 24.0 m, liquefied during the Pazarcık event. The grain size characteristics of surface ejecta also confirmed this conclusion. Back analyses of the rotational failure surfaces by limit equilibrium assessments revealed that the undrained residual strength of the liquefied silty sand layer varies in the range of 17 to 29.5 kPa. Similarly, the back-analyzed excess pore water pressure ratio value fall in the range of 0.85 to 0.91. Comparisons by available predictive models revealed that the liquefaction induced rotational failure of piled foundations and retaining system at the east abutment of Demirköprü bridge would be consistently predicted by any of the available residual shear strength or excess pore water pressure models.
Keywords: *Liquefaction, bridge, residual strength, sand volcanoes, failure*

Bu bildiride Demirköprü kazık temel elemanları ile dayanma yapılarında görülen ve zemin sıvılaşması sebebiyle tetiklenen dönme tipi yenilmeler tartışılacaktır. Sıvılaşma tetiklenme analizleri 8.0 ile 24.0 m, derinliklerde yer alan siltli kum birimlerinin Pazarcık depreminde sıvılaştığına işaret etmektedir. Yüzey sıvılaşma fışkırmalarından alınan numuneler üzerindeki dane dağılım deney sonuçları da bu görüşü desteklemektedir. Limit denge analizleri kapsamında gerçekleştirilen dairesel kayma yüzeylerinin geri analizi ile sıvılaşan siltli kum birimleri için artık kayma dayanım değerleri 17 ile 29.5 kPa aralığında hesaplanmıştır. Benzer olarak geri analizle bulunan aşırı boşluk suyu basınç oranı değerleri de 0.85 ile 0.91 aralığındadır. Tahmin denklemleri de bu değerlerle uyumlu sonuçlar ürettiğinden, Demirköprü kazık temel elemanlarında gözlenen zemin sıvılaşması sebepli dönme tipi yenilmelerin tahmin edilebileceği sonucuna varılmıştır.
Anahtar kelimeler: *Sıvılaşma, köprü, residüel mukavemet, kum fışkırması, yenilme*

1. INTRODUCTION

On February 6, 2023, two earthquakes, with moment magnitudes M7.8 and M7.6, triggered on the East Anatolian Fault Zone (EAFZ), at local times of 04:17 and 13:24, respectively. As shown in Figure 1, the epicenter of the first event, which has a focal depth of 8.6 km, is in Kahramanmaraş-Pazarcık. Kahramanmaraş-Pazarcık earthquake initiated approximately 20 km southeast of the main strand of the EAFZ along a splay fault, more specifically along Narlı fault, which is oriented in the northeast-southwest direction

[1] TUNGE Proje, ANKARA, socak@tungeproje.com, corresponding author
[2] Prof. Dr., Middle East Technical University, Department of Civil Engineering, ocetin@metu.edu.tr

(Melgar et al., 2023; Okuwaki et al., 2023, Petersen et al., 2023). The second event occurred approximately 9 hours later at a focal depth of 7.0 km in Kahramanmaraş-Elbistan-Ekinözü, 100 km north of the first event's epicenter, on an east-west-striking northern strand of the EAFZ: more specifically on the Sürgü-Misis fault zone (SMFZ). The resulting impact encompassed substantial casualties, injuries, and extensive infrastructure devastation. A total of 7 bridges were reported to be damaged after the earthquake series (Caner, Cetin and Gökceoglu, 2023).

Within the scope of this paper, liquefaction-induced failure of Demirköprü bridge is investigated. The soil liquefaction triggering, and post-liquefaction slope stability assessment results are presented herein. Back analyses of the rotational failure surfaces by limit equilibrium assessments enabled estimating the residual shear strength of liquefied soils. These back-calculated post liquefaction residual shear strength values are then compared with those of the predicted.

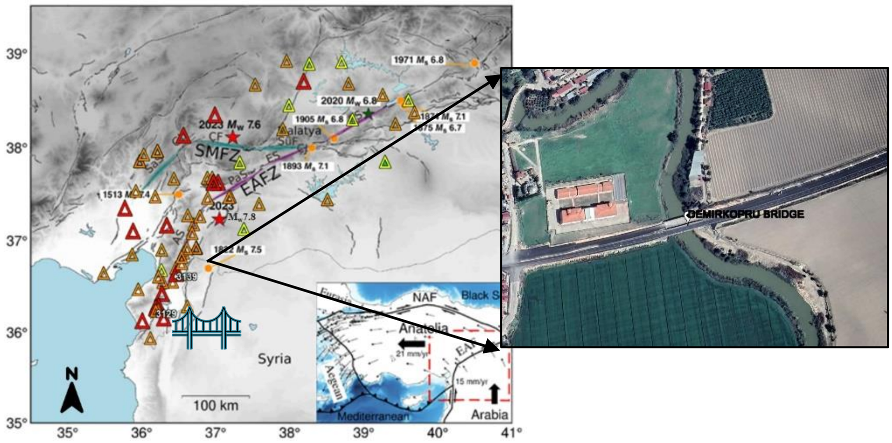

Figure 1: Map of the region showing fault systems (Duman and Emre, 2013) and major historical earthquakes (orange circles; Ambraseys, 1989) along EAFZ. Kahramanmaraş-Pazarcık earthquake ruptured the main segments of the EAFZ

2. SITE DESCRIPTION AND SEISMIC PERFORMANCE OF THE BRIDGE

Demirköprü bridge is in Demirköprü village of Antakya-Hatay at 36.246°N. 36.357°E. Figure 1 shows the location of the bridge. It is a three-span, prestressed reinforced concrete bridge, which serves as a passage over Asi River on Hatay – Reyhanlı state highway. Two twin bridges run parallel to each other. Each bridge has four piers, which are on piled foundations. More specifically, the middle piers are founded on 80 cm diameter, 18.5 long reinforced concrete bored piles. The abutment piers are 100 cm diameter, 21.5 long bored piles, designed for resisting loads applied by both the bridge and the approach embankment fill of 5.0 m high. It is observed during the site visits after the events that, the reinforced concrete bored piles in the east abutment tilted 20° towards Asi River, accompanied with settlements reaching as high as 1.0 to 1.5 m at the abutment embankment. Figure *2* shows the induced damage and widespread liquefaction-induced sand volcanoes mapped at the site. Six samples were taken from the ejecta soil and tested at METU Soil Mechanics Laboratory. The retrieved ejecta samples were classified as non-plastic silty sand (SM) with an average 25% fines content.

Figure 2 Induced damage and liquefaction induced ejecta due to Kahramanmaraş earthquake sequence

3. INTENSITY OF SHAKING LEVELS AT DEMIRKÖPRÜ BRIDGE SITE

AFAD, the national disaster and emergency management agency, operates 1548 strong ground motion stations nationwide. 280 of these stations were triggered during the Pazarcık M7.8 earthquake. Similarly, 244 SGMS recorded the second event.

Figure 3 presents the attenuation of the recorded PGA intensities with Joyner and Boore distance, Rjb, during both events. The Demirköprü bridge is located approximately 10 km and 200 km away from the fault rupture of the Pazarcık and Ekinözü-Elbistan events, respectively. Engineering assessments of liquefaction triggering and post-liquefaction residual shear strength are performed for the Pazarcık event and a soil PGA value of 0.45 g is adopted for Demirköprü Bridge within the scope of engineering assessments.

4. LIQUEFACTION ENGINEERING ASSESSMENTS

4.1. Site Investigations and Idealized Soil Profiles

A series of site investigation studies in the form of borings, disturbed and undisturbed sampling, in-situ (standard penetration test, SPT), and laboratory (soil classification, atterberg limit tests, etc.) tests were performed during the engineering design stage of the bridge. Boreholes BH – A and BH – B were conducted during the bridge construction phase only with SPT – N field values are available to be used. After the earthquake, 5 additional drillings (BH – 1 to 5) were made and laboratory test results could be obtained to be used in this study. The subsurface soil conditions along the cross-section exhibit a relatively consistent lateral pattern. At the ground surface of the site, Unit-1, a layer of low to high plasticity clay with occasional clayey sand lenses, is observed. The thickness of this layer varies from 2 to 9 meters. Typical field SPT blow counts, N values in this layer vary in the range of 2 – 5 blows/30 foot. Unit 2 underlies the surficial layer, which is defined as silty sand. The thickness of the layer varies from 20 to 30 meters. Typical field SPT blow counts, N values in silty sand layer vary in the range of 11 – 23 blows/30 foot. Unit 3, a 3 to 5m thick low plasticity clay layer, with field SPT-N values of 17 – 20, penetrated the silty sand layer at Elevations 73 to 78. Unit 4 is the deepest soil layer penetrated by borings, which is defined as low to high plasticity clay with SPT-N values of around 50. Table 1 summarizes available soil classification test results along with the representative SPT N values. In the same table, the representative Mohr-Coulomb shear strength parameters, which are to be used in the limit equilibrium assessments, are summarized.

5. LIQUEFACTION ENGINEERING ASSESSMENTS

5.1. Site Investigations and Idealized Soil Profiles

A series of site investigation studies in the form of borings, disturbed and undisturbed sampling, in-situ (standard penetration test, SPT), and laboratory (soil classification, atterberg limit tests, etc.) tests were performed during the engineering design stage of the bridge. Boreholes BH – A and BH – B were conducted during the bridge construction phase only with SPT – N field values are available to be used. After the earthquake, 5 additional drillings (BH – 1 to 5) were made and laboratory test results could be obtained to be used in this study. Table 1 summarizes available soil classification test results along with the representative SPT N values. In the same table, the representative Mohr-Coulomb shear strength parameters, which are to be used in the limit equilibrium assessments, are summarized.

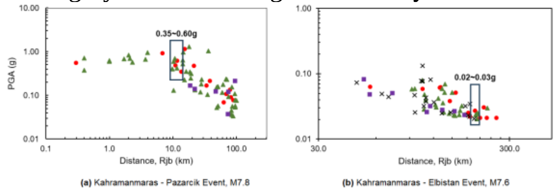

Figure 3 Joyner and Boore distance attenuation of PGAs recorded during the a) Pazarcık and b) Elbistan events

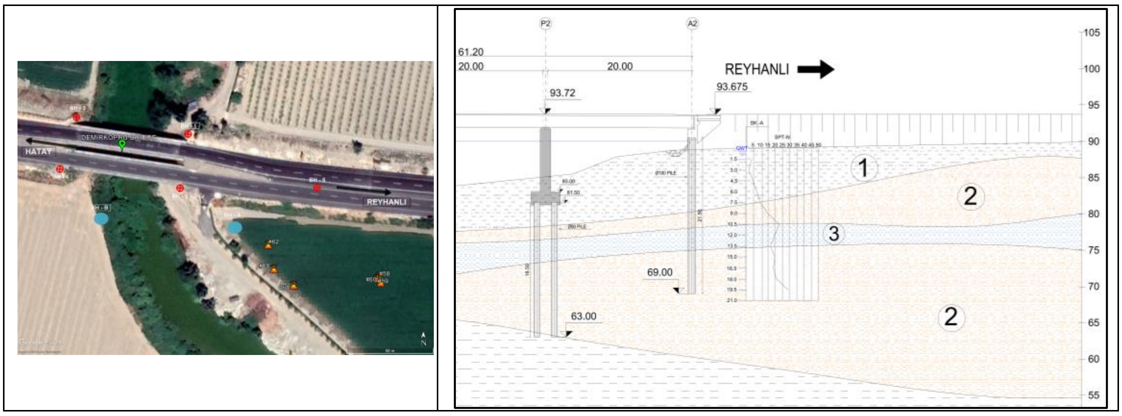

Figure 4 Plan view of the site showing the locations of site investigation studies along with representative subsurface cross sections. (1 - Low to High Plasticity Clay with clayey sand lenses, 2 - Non – Plastic Silty Sand, 3 - High Plasticity Clay)

5.2. Liquefaction Susceptibility and Triggering

The grain size characteristics of soil ejecta, and their comparisons with the characteristics of soil layers in the site revealed that the silty sand layer (Unit-2, SM layer) is the primary suspect soil layer of induced liquefaction. However, for the sake of completeness, the liquefaction susceptibility of other fine-grained soils are still assessed by (1) Seed et al. (2003), (2) Bray and Sancio (2006), Bilge and Cetin (2014) methods. Figure 6 clearly show that, except a few data points (less than 5 % of available data points), majority of fine-grained soils are classified as not susceptible, confirming the choice of suspect critical soil layer as silty sand (Unit 2, SM) layer. Seismic soil liquefaction triggering evaluations for non – plastic silty sands were performed for the soil profile that passes through the east abutment. As discussed earlier, the site-specific PGA value is estimated as 0.45g. Figure 6 presents the soil stratigraphy, including overburden, equipment, and procedure corrected SPT N1,60 values along with the values of factor of safety against liquefaction (FSliq). The FSliq values were estimated at each SPT depth by using Cetin et al. (2018) liquefaction triggering relationship. For the plastic layers that are evaluated to be non – liquefiable, a FSliq value of 2.0 is assigned.

5.3. Post Liquefaction Stability and Shear Strength

Back analyses are performed to estimate i) the residual undrained shear strength by using an undrained angle of shearing resistance ϕ_u value of 0 degrees in total stress analyses, ii) the induced excess pore pressure ratio (r_u) by using an angle of shearing resistance ϕ' value of 31 degrees in effective stress analyses. (Figure 7) The limit equilibrium-based back analyses, performed using Slide 6.020 software, results suggest a post liquefaction undrained residual shear strength value, varying in the range of 17 to 29.5 kPa, for the silty sand layer. Similarly, effective stress based back analyses results suggest cyclic excess pore pressure ratio (ru_{liq}) value, varying in the range of 0.85 to 0.91. These values are compared with the predictions by (1) Seed and Harder (1990), (2) Stark and Mesri (1992), (3) Idriss and Boulanger (2007), (4) Weber et al. (2015) and (5) Kramer, Wang (2015) and (6) Cetin and Bilge (2012) (Figure 8) As revealed by these comparison plots, the liquefaction induced rotational failure of piled foundations and

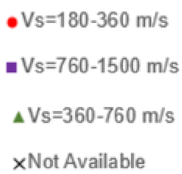

retaining system at the east abutment of Demirköprü bridge would be consistently predicted by all these predictive models.

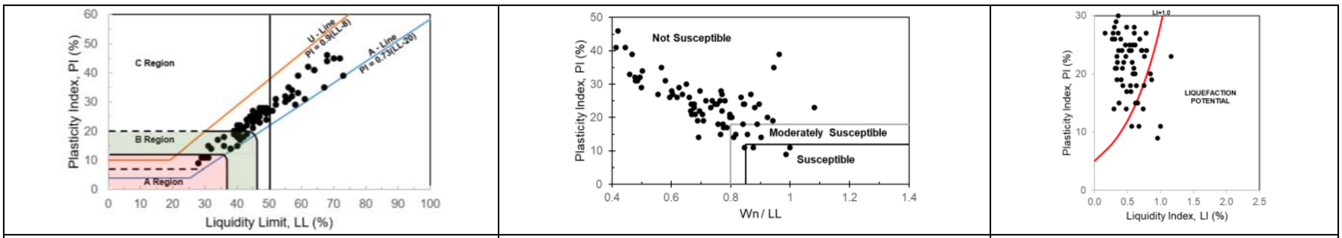

(a) Seed et al. (2003) | (b) Bray and Sancio (2006) | (c) Cetin and Bilge (2014)

Figure 5 Liuefaction - susceptibility assessment results for plastic soil particles

Table 1 Soil classification test results and the representative parameters assumed for limit equilibrium assessments.

Unit #	USCS	W_C (%)	LL (%)	PL (%)	PI (%)	LI (%)	FC (%)	SPT – N_{field}	γ (kN / m³)	Cu (kPa)	Ø (°)
1	SC CL CH	25.3* **35.5*** 30.6*	38.0 **61.0** 47.7	19.0 – 30.0 – 23.2	14.0 – 39.0 – 24.5	0.00 – 0.75 – 0.35	73 – 100 – 91	2 – 5 – 4	15.7	15	-
2	SM	NP					6 – 49 – 22	11 – 33 – 19	18.9	-	31
3	CH	22.9 – 39.1 – 33.0	44.0 – 70.0 – 53.4	18.0 – 25.0 – 21.6	24.0 – 45.0 – 31.9	-0.05 – 0.78 – 0.41	81 – 99 – 94	17 – 20 – 19	19.0	65	-
4	CL / CH	22.1 – 37.2 – 30.1	35.0 – 72.0 – 47.7	18.0 – 27.0 – 21.0	14.0 – 46.0 – 26.9	0.03 – 0.72 – 0.39	65 – 100 – 88	50	20.0	150	-

6. SUMMARY AND CONCLUSION

Liquefaction-induced failure of Demirköprü bridge, more specifically the rotational failure of the piled foundations and the retaining system of the eastern abutment, was discussed. The soil liquefaction triggering assessment results suggested that the silty sand layer located at depth range of 8.0 to 24.0 m, liquefied during the Pazarcık event. The grain size characteristics of surface ejecta also confirmed this conclusion. Both the triggering analyses and soil samples from soil ejecta confirm the suspect critical soil layer as silty sand (Unit 2, SM) layer. Back analyses are performed to estimate i) the residual undrained shear strength by using an undrained angle of shearing resistance ϕ_u value of 0 degrees in total stress analyses, ii) the induced excess pore pressure ratio (r_u). The results are compared with the well – known predictions in literature and it is evaluated that the liquefaction induced rotational failure of piled foundations and retaining system at the east abutment of Demirköprü bridge would be consistently predicted by all these predictive models.

REFERENCES

Stark, Timothy & Mesri, Gholamreza. (1992). Undrained Shear Strength of Liquefied Sands for Stability Analysis. Journal of Geotechnical Engineering. 118. 10.1061/(ASCE)0733-9410(1992)118:11(1727).

K.Onder Cetin, T.Leslie Youd, Raymond B Seed, Jonathan D Bray, Rodolfo Sancio, W Lettis, M.Tolga Yilmaz, H.Turan Durgunoglu, Liquefaction-induced ground deformations at Hotel Sapanca during Kocaeli (Izmit),Turkey earthquake, Soil Dynamics and Earthquake Engineering, Volume 22, Issues 9–12, 2002, Pages 1083-1092, ISSN 0267-7261, K Onder Cetin, Nihat Isik, Berna Unutmaz, (2004) “Seismically induced landslide at Degirmendere Nose, Izmit Bay during Kocaeli (Izmit) – Turkey earthquake, Soil Dynamics and Earthquake Engineering, Volume 24, Issue 3, 2004, Pages 189-197, ISSN 0267-7261,

Idriss, I.M., & Boulanger, R.W. (2007). SPT- and CPT-Based Relationships for The Residual Shear Strength of Liquefied Soils.

Cetin, K. O. & Bilge H. T. 2014. Recent advances in soil liquefaction engineering. Perspectives on European Earthquake Engineering and Seismology: Volume 1, edited by A. Ansal, Springer.

Cetin, K. O. and Bilge, H. T. (2012). “Cyclic Large Strain and Induced Pore Pressure Models for Saturated Clean Sands” J. Geotech. Geoenviron. Eng., 10.1061/(ASCE)GT.1943-5606.0000631 138:3(309), 309–323.

GEER (2023a) February 6, 2023 Türkiye Earthquakes: Report on Geoscience and Engineering Impacts. Geotechnical Extreme Event Reconnaissance Association (GEER), the Earthquake Engineering Research Institute, and the Earthquake Engineering Foundation of Türkiye. GEER Association Report 082. https://10.18118/G6PM34

GEER (2023b) February 6, 2023 Türkiye Earthquakes: GEER Phase 3 Team Report on Selected Geotechnical Engineering Effects. Geotechnical Extreme Event Reconnaissance Association, GEER Association Report 082-S1. https://doi.org/10.18118/G6F379

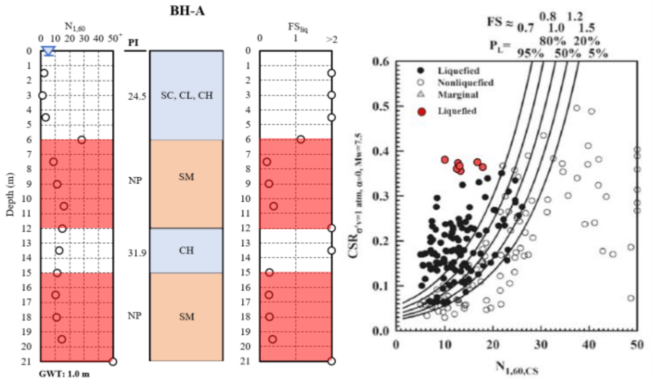

Figure 6 Liquefaction triggering assessment by using Cetin et al. (2018)

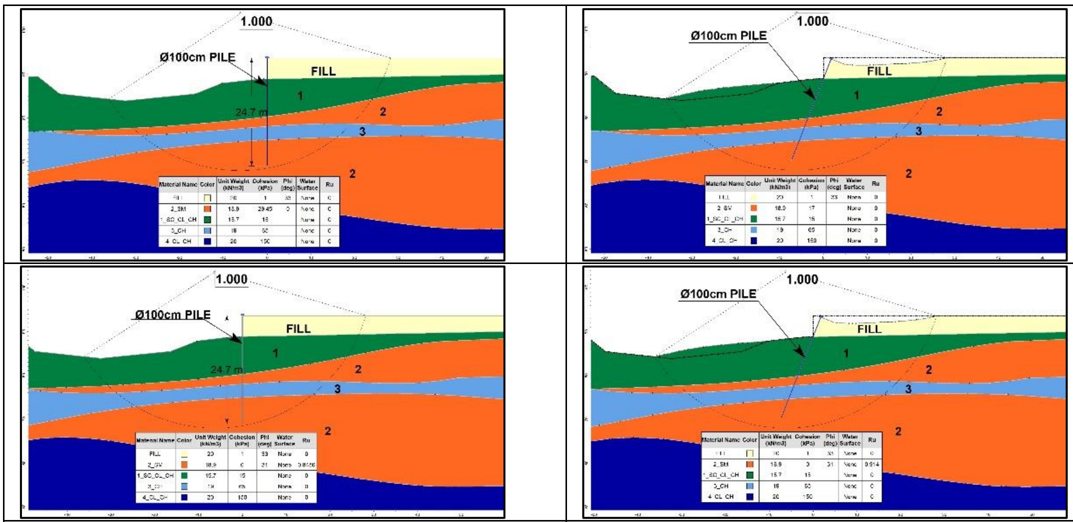

(a) Pre-failure geometry

(b) Post-failure geometry

Figure 7 Limit – equilibrium analyses results for the (a)pre-failure and (b) post-failure

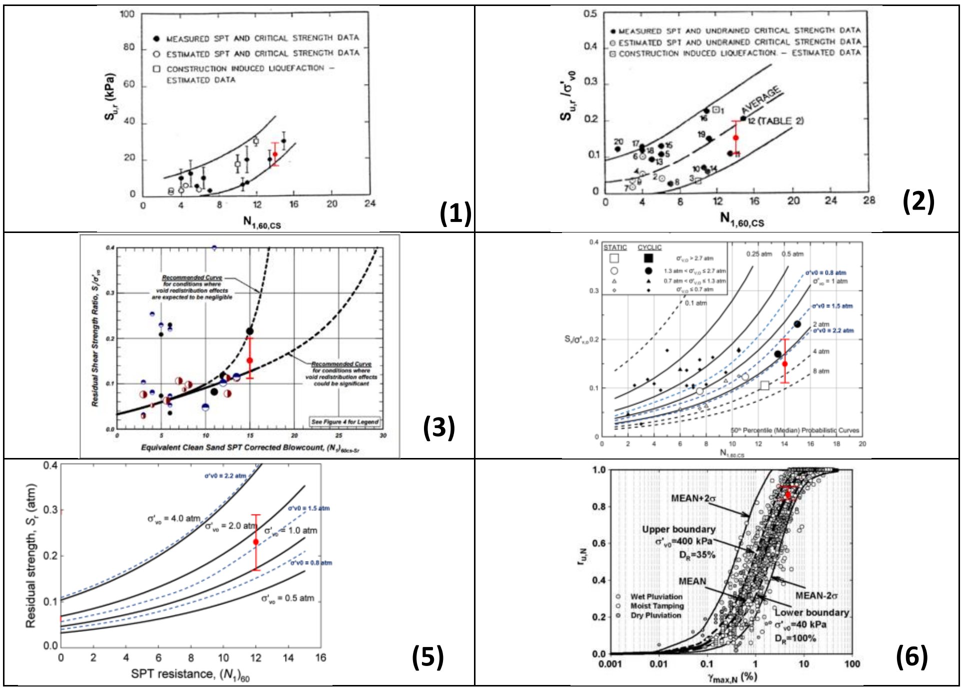

Figure 8 Illustrative comparisons of back-analyzed and predicted post liquefaction shear strength and excess pore water pressure responses.